Electronic Supplementary Material (ESI) for Nanoscale.

Supporting Information

Tunable UV-visible absorption of SnS_2 layered quantum dots produced by liquid phase exfoliation

Xiao Fu, [a] Pugazhendi Ilanchezhiyan, [a] Ganesan MohanKumar, [a] Hak D. Cho, [a] Lei Zhang, [c] Abdul S. Chan, [a] Dong J. Lee, [a] Gennady N. Panin,*, [a,b] Tae Won Kang*,[a]

[a.] *Quantum-Functional Semiconductor Research Center, Nano Information Technology Academy, Dongguk University, Seoul, 100-715, Republic of Korea*

[b.] *Institute of Microelectronics Technology and High-Purity Materials Russian Academy of Sciences, Chernogolovka, Moscow district, 142432, Russia*

[c.] *Hubei Collaborative Innovation Center for Advanced Organic Chemical Material Faculty of Materials Science Engineering, Hubei University, Wuhan 430062, China*

Section Ⅰ. Supporting Figures

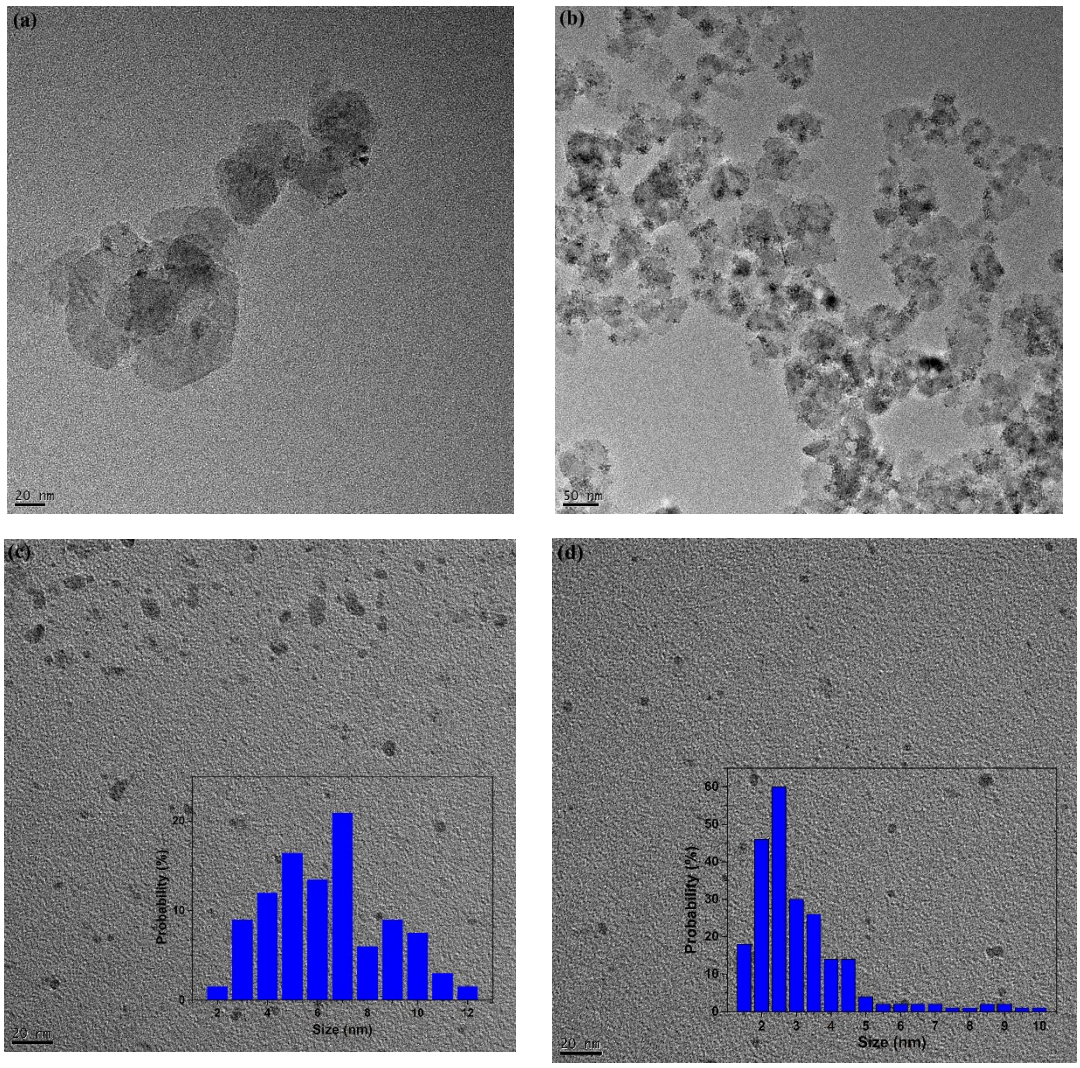

Figure S1. TEM images of SnS_2 layered nanocrystals obtained at 2000 (a) and 5000 rpm (b) and QDs obtained at 8000 (c) and 11000 rpm (d). Insets in (c) and (d) show the distributions of the quantum dots with the most detectable size from 4 to 7 nm and from 2 to 3 nm, respectively.

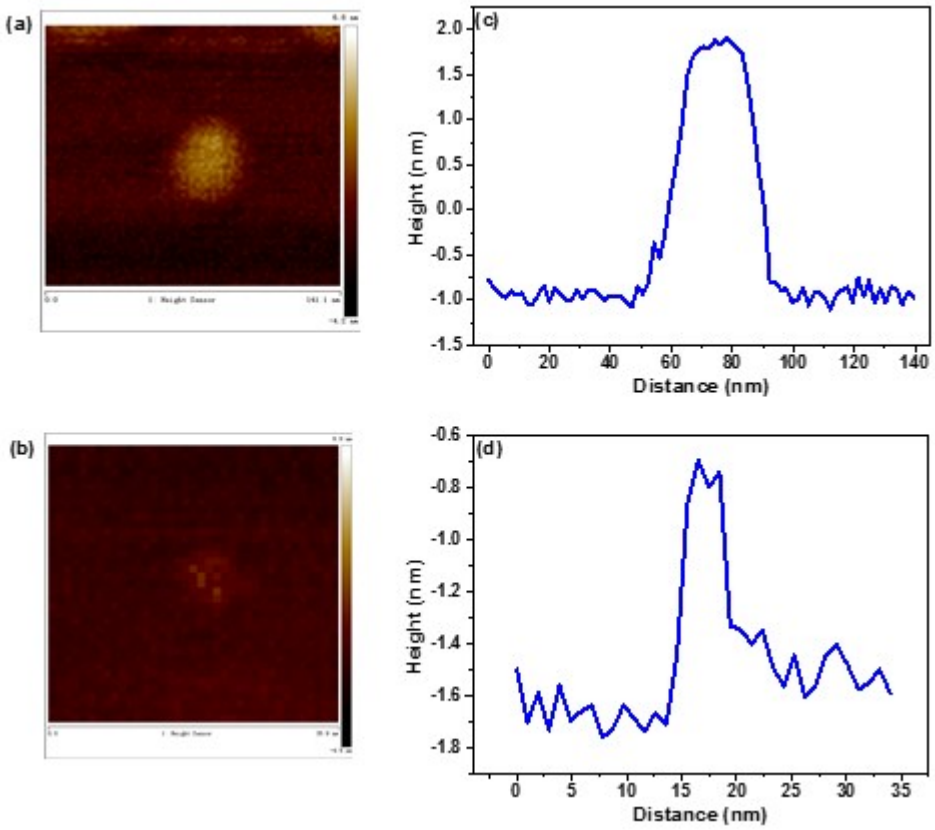

Figure S2. AFM images of a SnS_2 three-layer QD (a) and a SnS_2 single-layer QD (b) with their thickness profiles (c and d, respectively). The height of the single layer QD is around 0.8 nm, while the three-layer QD height is around 2.75 nm.

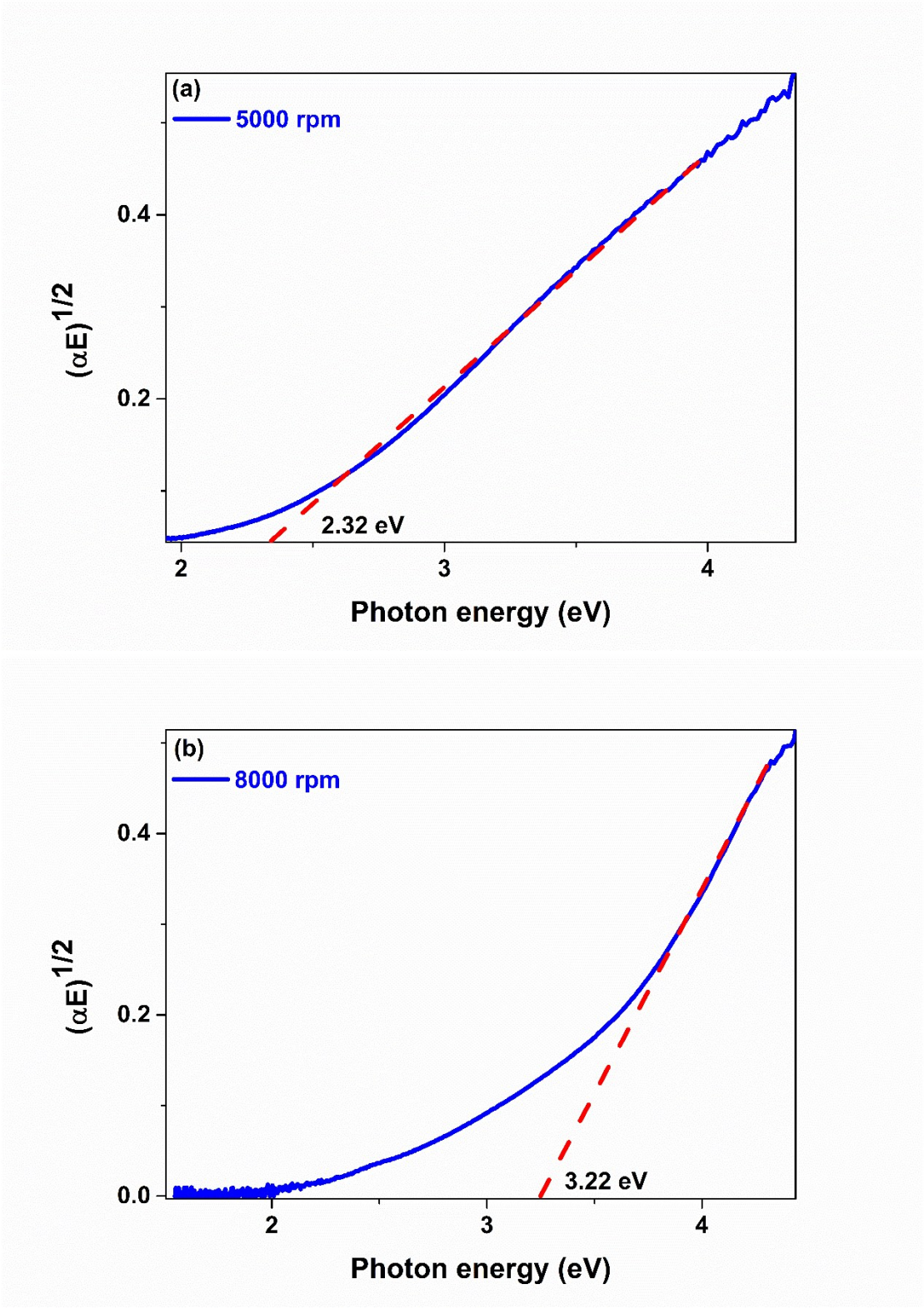

Figure S3. The plots of $(\alpha h\upsilon)^{1/2}$ vs $h\upsilon$ for the SnS_2 LQDs obtained at various speed of

centrifugation: a) 5000 rpm (E_g = 2.32 eV) and b) 8000 rpm (E_g = 3.22 eV).

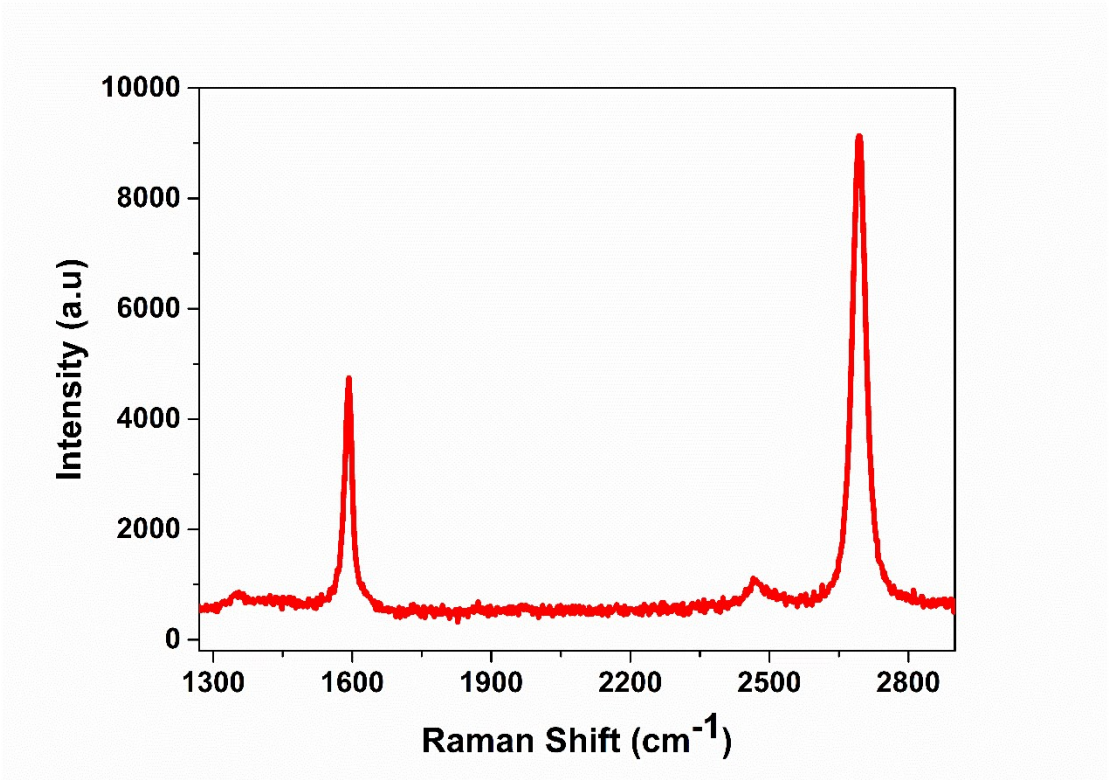

Figure S4. Raman spectra of graphene transferred on a SiO_2/Si substrate.

The electrode probes were fabricated from the transferred graphene layers grown on the Cu foil by CVD method at 1020°C in methane/hydrogen flow at 600 mTorr and used for photocurrent and tunneling current spectroscopy measurements. Raman scattering analysis was performed at room temperature using a 532 nm laser. The spectrum of graphene shows a weak D peak at 1355 cm^{-1}, indicating the high quality. The G and 2D peaks of graphene on SiO_2/Si are located at 1591 cm^{-1} and 2693 cm^{-1}, respectively. It shows the typical feature of monolayer graphene, with a full width at half maximum (FWHM) of 33.7 cm^{-1} for 2D peak and an $I_{(2D)}/I_{(G)}$ ratio of 2.13.

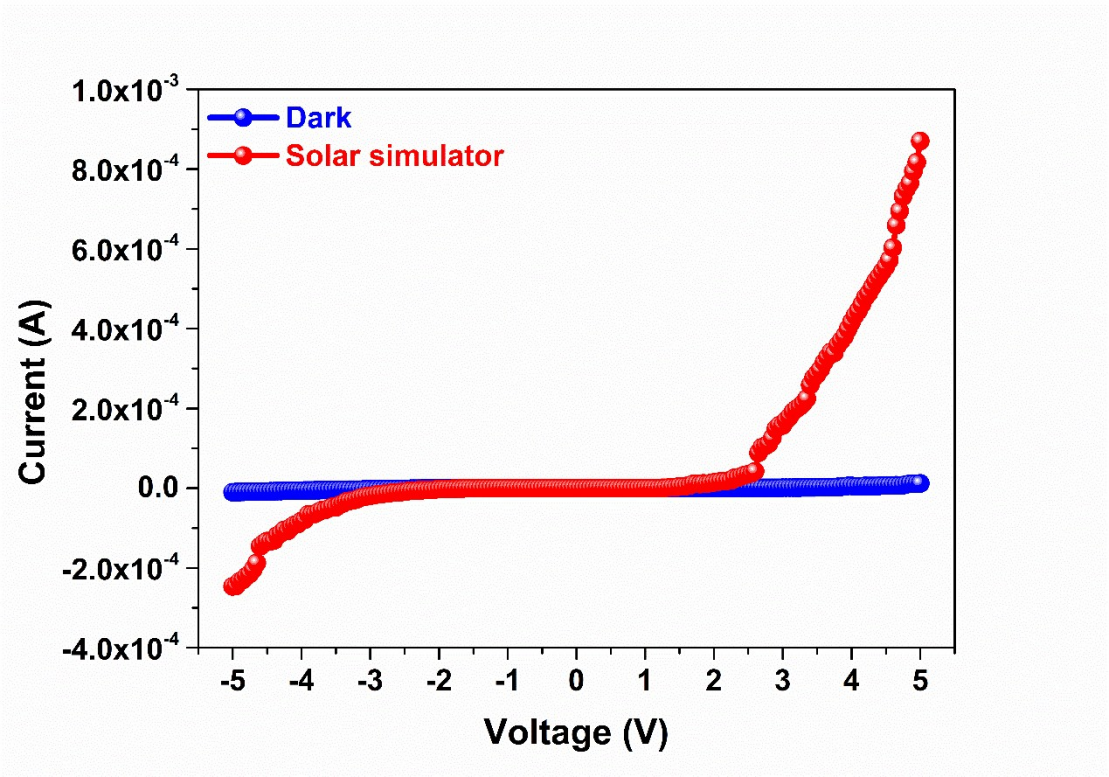

Figure S5. I-V curves of graphene/SnS_2 LQDs/graphene structure with LQDs of 2-90 nm in size (E_g =3.50 - 2.25 eV) in the dark and the sunlight with a solar simulator.

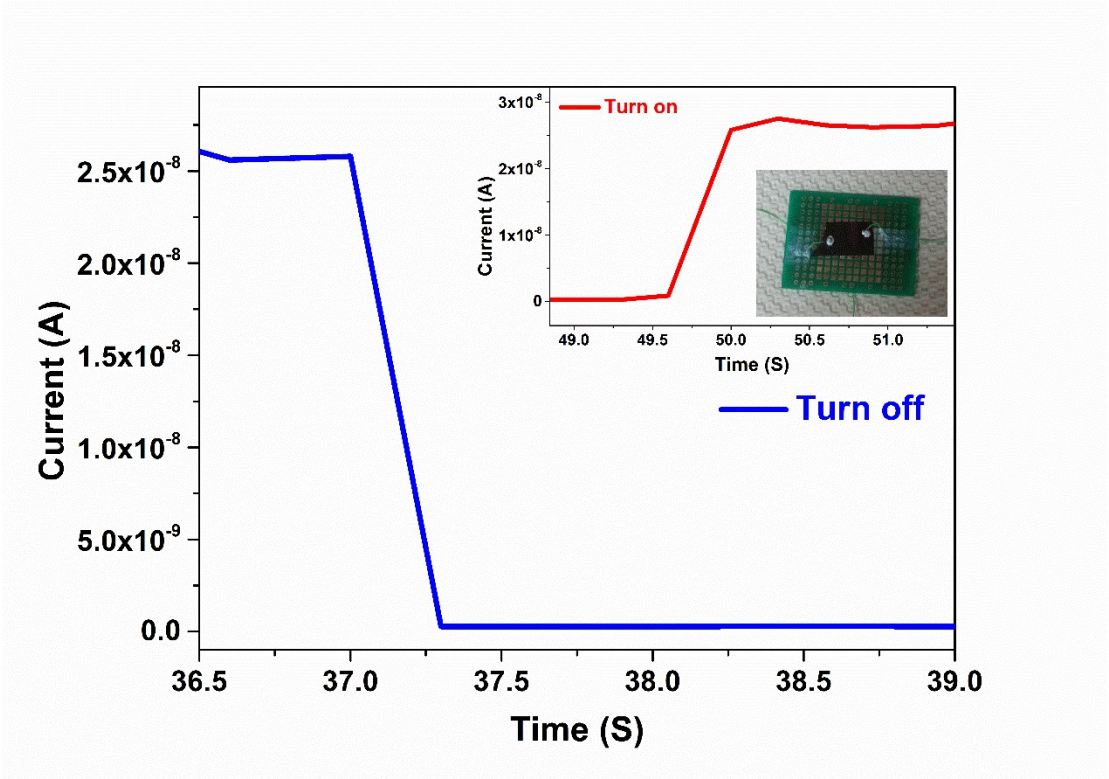

Figure S6. The dynamics of the photocurrent in SLQDs based device when switching off and turn on (inset) the light. Photograph of photodetector mounted on the measuring board is shown in the inset. The wires are attached to graphene electrodes placed of 10 microns apart on Si / SiO_2 substrate. The gap of 10 microns is filled by LQDs, as illustrated schematically in Fig. 4a and 4b. The measured time for decay and rise (333 ms) was limited to a maximum sampling rate used in our setup, which complicated the assessment of the actual rise and decay times of photodetectors made of quantum dots with different sizes.

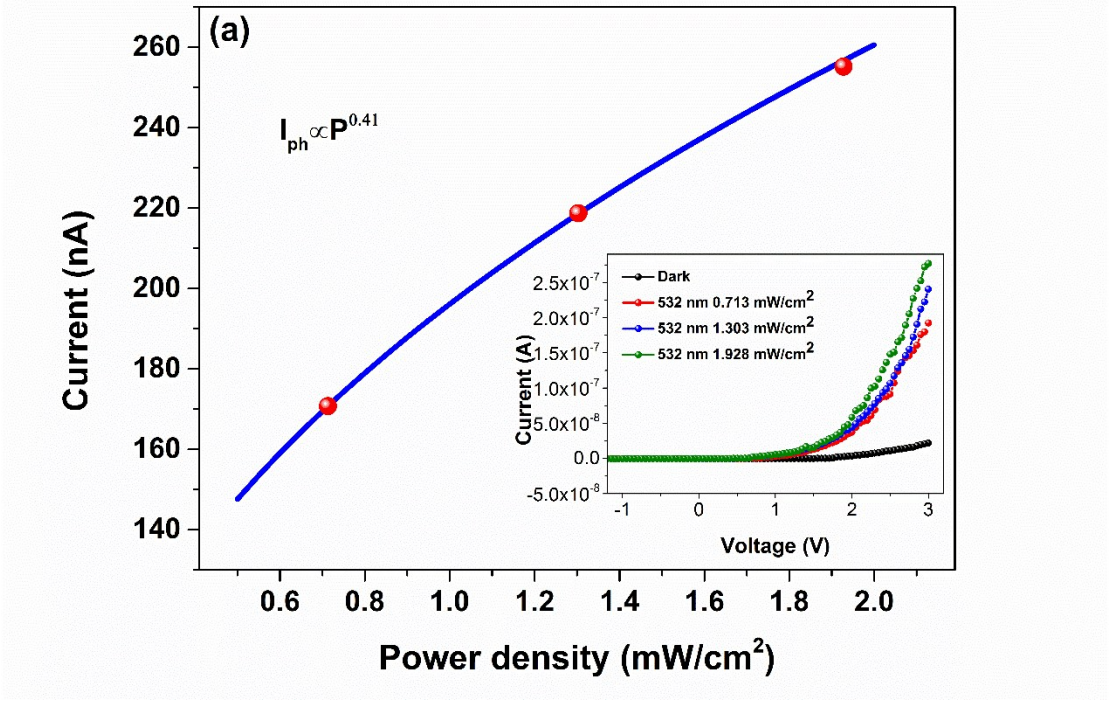
(a)
$I_{ph} \propto P^{0.41}$
Current (nA)
Power density (mW/cm^2)
Dark
532 nm 0.713 mW/cm^2
532 nm 1.303 mW/cm^2
532 nm 1.928 mW/cm^2
Current (A)
Voltage (V)

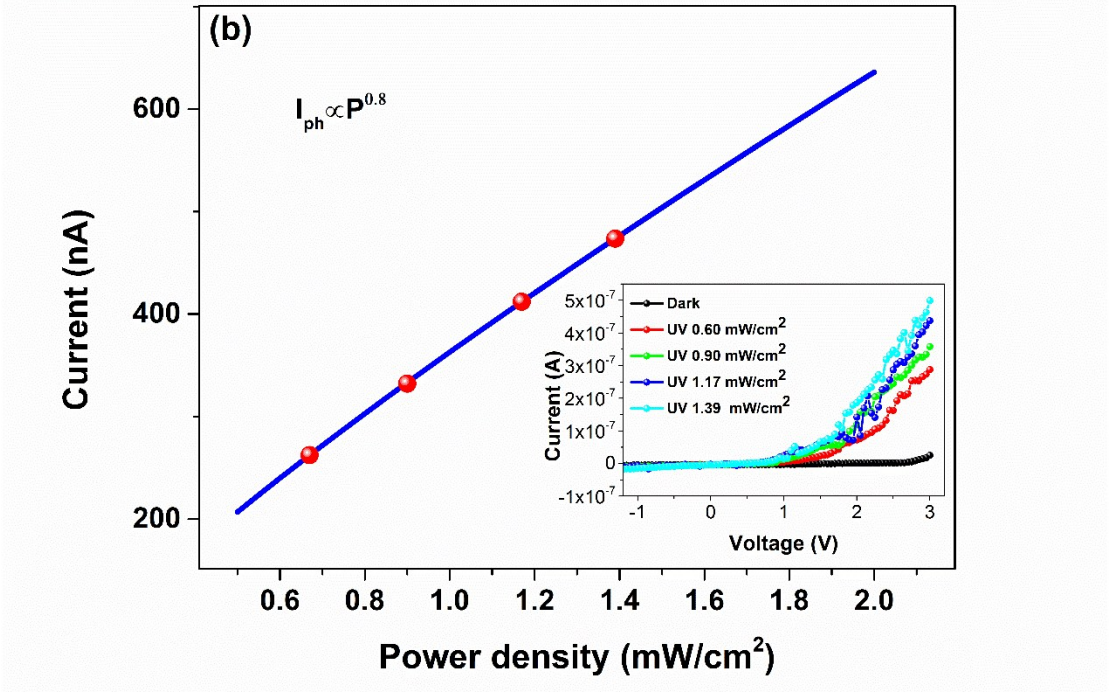
(b)
$I_{ph} \propto P^{0.8}$
Current (nA)
Power density (mW/cm^2)
Dark
UV 0.60 mW/cm^2
UV 0.90 mW/cm^2
UV 1.17 mW/cm^2
UV 1.39 mW/cm^2
Current (A)
Voltage (V)

Figure S7. Photocurrent as a function of illumination intensity for the graphene/SnS_2 nanocrystals-LQDs/graphene structure with LQDs of 2-40 nm in size. Inset shows the I-V curves of the structure in the dark and under 532 nm light (a) and UV radiation (b). As the incident light intensity increases, the photocurrent also increases, resulting in a positive relationship between the carrier photogeneration efficiency and the absorption of the incident light. This correlation can be described by a power law: $I_{ph} \propto P^{\theta}$, where θ reflects the photocurrent efficiency. Fitting the curve, as shown in Fig. S7, leads to the value of θ= 0.41 for 532 nm light and 0.8 for UV-radiation.

Section Ⅱ.

Tunneling current spectroscopy has been used to provide information about the surface density of states in semiconductor as a function of their energy.

Using the modified Bardeen transfer Hamiltonian method, which treats tunneling as a perturbation, the tunneling current (I) is:

$$I = \frac{4\pi e}{\hbar}\int_{-\infty}^{\infty}[f(E_f - eV + \epsilon) - f(E_f + \epsilon)]\rho_s(E_f - eV + \epsilon)\rho_T(E_f + \epsilon)|M_{\mu\nu}|^2 d\epsilon \quad . (1)$$

Where $f(E)$ is Fermi distribution function, ρ_s and ρ_T are the density of states in the sample and tip, respectively, $M_{\mu\nu}$ is the tunneling matrix element between the modified wavefunctions of the tip and the sample surface. The tunneling matrix element.

For a constant tunneling matrix element, the tunneling current reduces to:

$$I \propto \int_{0}^{eV}\rho_s(E_f - eV + \epsilon)\rho_T(E_f + \epsilon)d\epsilon. \quad (2)$$

Differentiation dI/dV determines the energy dependence of density of states:

$$\frac{dI}{dV} \propto \rho_s(E_f - eV) \quad . \quad (3)$$

Here we use the biased (-3.5-3.5 V) graphene tip of atomic scale (0.6 nm) which can produce locally a high electric field (> 10^6 V/cm) at an interface vdW gap (4-6Å) [1, 2].

The vdW gap between graphene and 2D SnS_2 controls the tunneling current induced by biased voltage in both directions that gives possibility to estimate electrically the bandgap of the LQDs (Fig. 5a).

References:

1.T. Roy, M. Tosun, X. Cao, H. Fang, D Lien, P. Zhao, Y. Chen, Y. Chueh, J. Guo, and Ali Javey, *ACS Nano,* **2015**, 9, 2071−2079.

2. Y. Cao, A. Mishchenko, G. L. Yu, E. Khestanova, A. P. Rooney, E. Prestat, A. V. Kretinin, P. Blake, M. B. Shalom, C. Woods, J. Chapman, G. Balakrishnan, I. V. Grigorieva, K. S. Novoselov, B. A. Piot, M. Potemski, K. Watanabe, T. Taniguchi, S. J. Haigh, A. K. Geim and R. V. Gorbachev, *Nano Lett*, **2015**, 15 (8), 4914–4921.